Dynamics of quantum coherence in a spin-star system: Bipartite initial state and coherence distribution

Chandrashekar Radhakrishnan,[1,2] Zhiguo Lü,[3,4,*] Jun Jing,[5,†] and Tim Byrnes[6,1,2,7,8,‡]

[1]*New York University Shanghai, 1555 Century Ave, Pudong, Shanghai 200122, China*

[2]*NYU-ECNU Institute of Physics at NYU Shanghai, 3663 Zhongshan Road North, Shanghai 200062, China*

[3]*Key Laboratory of Artificial Structures and Quantum Control (Ministry of Education), School of Physics and Astronomy, Shanghai Jiao Tong University, Shanghai 200240, China*

[4]*Collaborative Innovation Center of Advanced Microstructures, Nanjing 210093, China*

[5]*Department of Physics, Zhejiang University, Hangzhou 310027, Zhejiang, China*

[6]*State Key Laboratory of Precision Spectroscopy, School of Physical and Material Sciences, East China Normal University, Shanghai 200062, China*

[7]*National Institute of Informatics, 2-1-2 Hitotsubashi, Chiyoda-ku, Tokyo 101-8430, Japan*

[8]*Department of Physics, New York University, New York, New York 10003, USA*

(Received 30 April 2019; published 31 October 2019)

We investigate the transient dynamics of quantum coherence for a system of two central spins in a spin-star environment by employing a numerical procedure based on a Laguerre polynomial expansion scheme. The dynamics of the total, local, and global coherence are calculated for different values of the anisotropy parameter, the system-bath interaction strengths, and temperature for different initial bipartite states. Significant dynamical features of quantum coherence are found as follows: (i) an X state can only have global coherence; (ii) a state with only initial local coherence gains global coherence during the course of evolution by the induced correlations between the two-qubit system and the common bath; (iii) an incoherent state gains coherence by interacting with an external bath. We find there are two primary ways to gain coherence for an incoherent state: one is by interacting with the external quantum bath and the other is through interconversion of other quantum properties such as purity into coherence. Finally, we demonstrate that our results for the system in an infinite bath also hold qualitatively when the system is in contact with a finite bath.

DOI: 10.1103/PhysRevA.100.042333

I. INTRODUCTION

The field of quantum information science has shown numerous advantages of using quantum mechanics over classical physics in technological applications, such as with quantum computing algorithms, quantum metrology, quantum simulation, and quantum cryptography. This improvement is due to the utilization of coherent quantum resources such as entanglement and superposition. In any realistic situation, the quantum computer will possess various channels of decoherence, due to their interaction with the external environment and hence such systems should be considered as open quantum systems. One of the best investigated quantum resources in the context of quantum information processing is entanglement. While an essential ingredient for many quantum information processing tasks, it has become more apparent in recent years that it is not the only quantum resource that can be exploited, and there are several other quantum resources such as discord [1,2], coherence [3], steering [4], and contextuality [5], which can be used for various applications.

Coherence is a well-known feature of quantum mechanics since the concept of wave-particle duality was first introduced. While it was studied intensively in the context of phase-space distributions and higher-order correlation functions, it was never quantified in a rigorous sense in terms of a quantum information quantity. This was performed recently by Baumgratz, Cramer, and Plenio [3], and improved upon by many subsequent works focused on measuring and distribution of quantum coherence [3,6–14]. It has also been investigated in a wide variety of systems like Bose-Einstein condensates [15], cavity electrodynamics [16], and spin systems [17–20].

Recently, there have been many advancements in qubit technology for various systems [21]. In particular, for qubits made using quantum dots [22,23] and NV centers [24], the qubit system is located in a solid-state medium which contains many other spin systems such as the nuclear spins of the host material. This naturally leads to a very complex interaction between the qubit and the neighboring spin systems, which may also be mutually interacting. Due to the complex dynamics induced by the spin environment on the qubits, still a lot of work has to be done to completely understand the dynamics of NV centers and quantum dots [25]. In general, in solid state devices such as quantum dots and NV centers there is background noise due to the presence of nuclear spins. The qubit-nuclear spin system can be modeled as a central

*zglv@sjtu.edu.cn
†jingjun@zju.edu.cn
‡tim.byrnes@nyu.edu

spin in contact with a spin bath. The transient dynamics of entanglement in such systems has been studied using several techniques such as perturbative methods [26] and mean-field approximation [27]. In Ref. [28], the dynamics of a central spin coupled to a spin-star network through a Heisenberg XX coupling was studied. This was extended to two central spins in Ref. [29]. The entanglement dynamics of a very general Heisenberg XY model was solved using an operator technique in Ref. [30]. Later a semianalytic model was introduced in Refs. [31–33] to investigate the dynamics of entanglement in the anisotropic XY model for an arbitrary initial state. This model has wide applications in several quantum information processing systems such as quantum dots and cavity QED [34–37].

In this paper, we investigate the dynamics of an open two spin qubit system in a spin-star network with a homogenous coupling to the environment spins. We consider the two spins to be separated sufficiently that the direct spin-spin coupling between them can be neglected. Through the use of Holstein-Primakoff transformation we convert our model to a spin-boson Hamiltonian, and compute the dynamics of the two central spins through a numerical simulation assuming different pure and mixed initial states. The dynamics of quantum coherence is measured using the relative entropy of coherence [3]. The coherence is decomposed into contributions arising due to correlations between the qubits or locally, called the global coherence and local coherence [8,38], respectively. The manuscript is organized as follows. In Sec. II and Sec. III we describe the spin model and the coherence measure, respectively. The numerical techniques are explained in detailed in Sec. IV. The dynamics of pure states are analyzed through the study of the Bell states, coherent separable state, and incoherent separable state in Sec. V. The mixed states are considered in Sec. VI through the investigation of Werner-Bell states, mixed separable state, and the maximally mixed states. We present our conclusions in Sec. VII.

II. DESCRIPTION OF THE MODEL

We consider a two-qubit subsystem interacting with an external bath, where both the subsystem and the bath are composed of two level systems. The spin-star configuration is a structure in which the two-qubit subsystem is surrounded by N-spin particles located on the surface of a sphere. The spins in the subsystem interact with the bath spins through a Heisenberg XY-type interaction. In addition, the bath spins interact between themselves through an XY spin interaction. Here we assume that each spin in the bath interacts with the two central spins with equal strengths, similar to that discussed in Refs. [28,30,39,40]. The Hamiltonian corresponding to the total system comprising the spin subsystem and the spin bath can be decomposed into three parts

$$H = H_S + H_{SB} + H_B, \tag{1}$$

where H_S and H_B are the Hamiltonians of the subsystem and the bath, respectively, while H_{SB} describes the interaction between the bath and the subsystem. In terms of the spin operators, the Hamiltonians H_S, H_B, and H_{SB} read

$$H_S = \mu_0\left(\sigma_{01}^z + \sigma_{02}^z\right), \tag{2}$$

$$H_{SB} = \frac{g_0}{2\sqrt{N}}\sum_{i=1}^{N}\left[(1+\gamma)\left(\sigma_{01}^x\sigma_i^x + \sigma_{02}^x\sigma_i^x\right) + (1-\gamma)\left(\sigma_{01}^y\sigma_i^y + \sigma_{02}^y\sigma_i^y\right)\right], \tag{3}$$

$$H_B = \frac{g}{2N}\sum_{i\neq j}^{N}\left[(1+\gamma)\sigma_i^x\sigma_j^x + (1-\gamma)\sigma_i^y\sigma_j^y\right], \tag{4}$$

where the $\sigma_i^{x,y,z}$ represents the Pauli spin operators and the index i runs from 1 to N, where N is the number of spins in the bath. Here $\sigma_{01}^{x,y,z}$ ($\sigma_{02}^{x,y,z}$) represents the Pauli spin operator corresponding to the first (second) spin of the system. The coupling between the system and any bath spin is g_0, while g is the coupling between the bath spins. The factor μ_0 describes the coupling between the spin qubit and the external field in the $\hat{Z}$ direction. The anisotropy parameter has a range $\gamma \in [-1, 1]$, where $\gamma = 0$ means the interaction is of an isotropic case and $\gamma = 1$ represents a strong anisotropic case (Ising type interaction). The spin-star environment is symmetric in the parameter γ about the point $\gamma = 0$ and hence we will consider only the regime $\gamma \in [0, 1]$.

The interaction Hamiltonian and the bath Hamiltonian can be rewritten using the spin raising and lowering operators $\sigma^{\pm} = (\sigma^x \pm i\sigma^y)/2$ as

$$H_{SB} = \frac{g_0}{\sqrt{N}}\left[\sum_{i=1}^{N}\sigma_i^+(\gamma\sigma_{01}^+ + \sigma_{01}^-) + \sum_{i=1}^{N}\sigma_i^-(\sigma_{01}^+ + \gamma\sigma_{01}^-) + \sum_{i=1}^{N}\sigma_i^+(\gamma\sigma_{02}^+ + \sigma_{02}^-) + \sum_{i=1}^{N}\sigma_i^-(\sigma_{02}^+ + \gamma\sigma_{02}^-)\right], \tag{5}$$

$$H_B = \frac{g}{N}\sum_{i\neq j}^{N}[\gamma(\sigma_i^+\sigma_j^+ + \sigma_i^-\sigma_j^-) + (\sigma_i^+\sigma_j^- + \sigma_i^-\sigma_j^+)]. \tag{6}$$

Due to the symmetric coupling of the bath spin operators, we can introduce the collective angular momentum operator $J_{\pm} = \sum_{i=1}^{N}\sigma_i^{\pm}$. Substituting $J_{\pm}$ into (5) and (6), we get

$$H_{SB} = \frac{g_0}{\sqrt{2j}}[J_+(\gamma\sigma_{01}^+ + \sigma_{01}^-) + J_-(\gamma\sigma_{01}^+ + \sigma_{01}^-) + J_+(\gamma\sigma_{02}^+ + \sigma_{02}^-) + J_-(\gamma\sigma_{02}^+ + \sigma_{02}^-)], \tag{7}$$

$$H_B = \frac{g}{2j}[\gamma(J_+J_+ + J_-J_-) + (J_+J_- + J_-J_+ - 2j)], \tag{8}$$

where $j = N/2$. Now we perform a Holstein-Primakoff transformation [41]

$$J_+ = b^\dagger(\sqrt{2j - b^\dagger b}), \quad J_- = (\sqrt{2j - b^\dagger b})b, \tag{9}$$

to transform the collective angular momentum operators to bosonic operators b, obeying bosonic commutation relations

$[b, b^\dagger] = 1$. The Hamiltonians (7) and (8) can be recast as

$$H_{SB} = g_0\Bigg[b^\dagger\sqrt{1-\frac{b^\dagger b}{N}}(\gamma\sigma_{01}^+ + \sigma_{01}^- + \gamma\sigma_{02}^+ + \sigma_{02}^-) + \sqrt{1-\frac{b^\dagger b}{N}}b(\sigma_{01}^+ + \gamma\sigma_{01}^- + \sigma_{02}^+ + \gamma\sigma_{02}^-)\Bigg], \tag{10}$$

$$H_B = g\Bigg[\gamma\left(b^\dagger\sqrt{1-\frac{b^\dagger b}{N}}\,b^\dagger\sqrt{1-\frac{b^\dagger b}{N}} + \sqrt{1-\frac{b^\dagger b}{N}}b\sqrt{1-\frac{b^\dagger b}{N}}b\right) + b^\dagger\left(1-\frac{b^\dagger b}{N}\right)b + \sqrt{1-\frac{b^\dagger b}{N}}bb^\dagger\sqrt{1-\frac{b^\dagger b}{N}} - 1\Bigg]. \tag{11}$$

In the thermodynamic limit $N \to \infty$, Eqs. (10) and (11) can be well approximated by

$$H_{SB} = g_0[b^\dagger\,(\gamma\sigma_{01}^+ + \sigma_{01}^- + \gamma\sigma_{02}^+ + \sigma_{02}^-) + b\,(\sigma_{01}^+ + \gamma\sigma_{01}^- + \sigma_{02}^+ + \gamma\sigma_{02}^-)], \tag{12}$$

$$H_B = g[\gamma(b^{\dagger 2} + b^2) + 2b^\dagger b]. \tag{13}$$

Thus we find that the initial Hamiltonian describing a two-qubit spin system in a spin-star environment is transformed to a Hamiltonian describing a two-qubit system interacting with a single-mode thermal bosonic bath field. This can be equally considered to be a nontrivial problem in cavity quantum electrodynamics.

III. MEASUREMENT OF QUANTUM COHERENCE

We now turn to analyzing the dynamics of coherence of the bipartite spin system immersed in a common spin environment, as described by the Hamiltonian in the last section. To investigate the quantum coherence we use the relative entropy of coherence measure given by [3]

$$C_T(\rho_s) = \min_{\sigma\in\mathcal{I}} S(\rho_s\|\sigma) = S(\rho^d) - S(\rho_s), \tag{14}$$

where we denote the set of incoherent states by $\mathcal{I}$ and ρ^d is the diagonal matrix corresponding to the density matrix of the two-qubit subsystem ρ_s. The coherence quantified by (14) is the total coherence of the subsystem. Unlike entanglement, coherence can either be localized within the qubits (local coherence) or may exist as correlations between the qubits (global coherence) [8]. The local coherence can be measured using the relation

$$C_L = S(\pi(\rho_s)\|[\pi(\rho_s)]^d), \tag{15}$$

where $\pi(\rho_s) = \rho_1 \otimes \rho_2$ is the product state of the two central spins and $\rho_{1,2} = \mathrm{Tr}_{2,1}\rho_s$. The global coherence can be found from the total coherence (14) and the local coherence (15) by considering their difference

$$C_G = C_T - C_L. \tag{16}$$

IV. NUMERICAL CALCULATION PROCEDURE

We now describe the numerical methods used in this work to find the time evolved density matrix $\rho(t)$ from an initial density matrix. We take the initial density matrix to be of the form

$$\rho(0) = \rho_s(0) \otimes \rho_B(0), \tag{17}$$

where $\rho_s(0) = |\psi(0)\rangle\langle\psi(0)|$ and $\rho_B(0)$ are the initial density matrices corresponding to the two-qubit spin subsystem and the spin environment, respectively.

We assume the external bath is initially at thermal equilibrium, such that it obeys the Boltzmann distribution

$$\rho_B(0) = \frac{\exp(-H_B/k_BT)}{Z}, \tag{18}$$

where $Z = \mathrm{Tr}\exp(-H_B/k_BT)$ is the partition function of the bath. For the sake of simplicity, we use units of energy and temperature such that $k_B = 1$. The time evolved density matrix of the entire system can be computed through the expression

$$\rho(t) = \exp(-iHt)\rho(0)\exp(+iHt). \tag{19}$$

To find the time evolved density matrix $\rho(t)$, we adopt the procedure introduced in Ref. [42]. Here the thermal bath state $\rho_B(0)$ is expanded in terms of the eigenstates of the environment Hamiltonian H_B as follows:

$$\rho_B(0) = \sum_{m=1}^{M}\omega_m|\phi_m\rangle\langle\phi_m|, \tag{20}$$

where $|\phi_m\rangle$, $m = 1, \ldots, M$ are the eigenstates of H_B with corresponding eigenenergies E_m. The Boltzmann weight ω_m reads

$$\omega_m = \frac{\exp(-E_m/T)}{Z}, \qquad Z = \sum_{m=1}^{M}\exp(-E_m/T). \tag{21}$$

In the above discussion the index M represents the total number of eigenstates. Since we used a Holstein-Primakoff transformation to convert the spin bath to a single mode thermal bath field, for consistency we must take the $M \to \infty$ limit. For energy states with $E_m/T \gg 1$, the Boltzmann factor is negligible and thus we may approximate the bath state in practice with a cutoff m_c:

$$\rho_B(0) \approx \sum_{m=1}^{m_c}\omega_m|\phi_m\rangle\langle\phi_m|. \tag{22}$$

Taking into account all these considerations we can write the density matrix $\rho(t)$ as

$$\rho(t) = \sum_{m=1}^{m_c}\omega_m|\Psi_m(t)\rangle\langle\Psi_m(t)|, \tag{23}$$

where

$$|\Psi_m(t)\rangle = \exp(-iHt)|\Psi_m(0)\rangle = U(t)|\Psi_m(0)\rangle, \tag{24}$$

and the initial state is

$$|\Psi_m(0)\rangle = |\psi(0)\rangle|\phi_m\rangle. \tag{25}$$

Now we find the evolution operator $U(t)$, which describes the dynamics of the two qubit central spins. There are several different methods to find the evolution operator. An operator

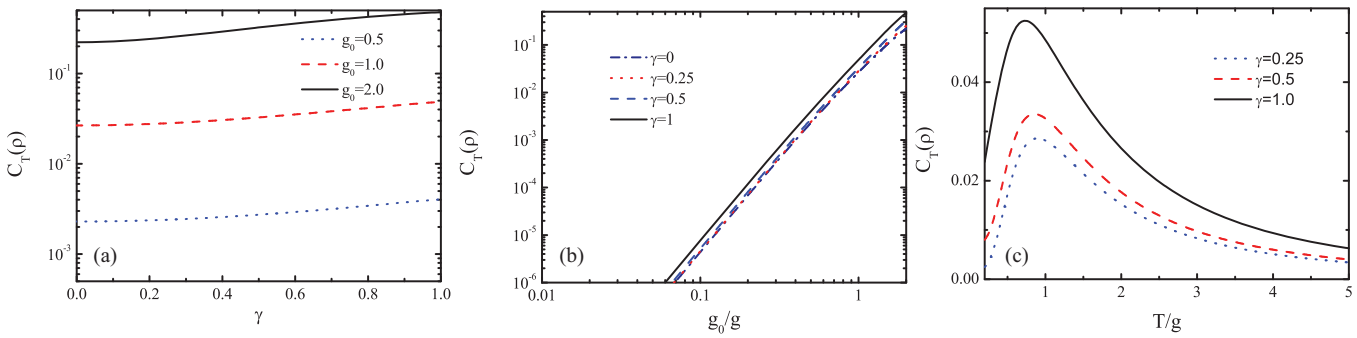

FIG. 1. Coherence of the steady state corresponding to $\rho(t \to \infty)$ is given above for $\mu_0 = 2g$ and $g = 1$. In (a) we calculate the variation of coherence with γ for different values of g_0 keeping $T = g$. The variation of coherence with respect to g_0/g is given in (b) for different values of γ and the value of $T = g$. The coherence variation with respect to temperature is given in (c) for different values of γ and $g_0 = g$.

based technique was introduced in Ref. [30] to study the dynamics of X states. An alternative to this is to use a polynomial based scheme, which was introduced in Ref. [43] and further developed in Ref. [44]. In the current work we use the Laguerre polynomial based expansion method introduced in Ref. [45] and used extensively in Ref. [46]. This method is suitable for many quantum systems and can give accurate results with much smaller computational overhead. The evolution operator based on the Laguerre polynomial of the Hamiltonian is

$$U(t) = \left(\frac{1}{1+it}\right)^{\alpha+1} \sum_{k=0}^{\infty} \left(\frac{1}{1+it}\right)^{k} L_k^{\alpha}(H). \tag{26}$$

Here $L_k^{\alpha}(H)$ is the Laguerre polynomial of type α and H is the Hamiltonian. The index $\alpha \in (-1, \infty)$ distinguishes different types of Laguerre polynomials and k is its order. In the case of a spin-star environment we take $\alpha = -1/2$, while for other models it can have different values with regard to the numerical convergence speed [46]. Though the order of the Laguerre polynomial $k \to \infty$, in actual calculations we truncate this to $k_{\max}$, an optimal value. In our present work we choose this optimal value through an investigation of the numerical stability in the recurrence of the Laguerre polynomial and the speed of the calculation. Once the order of the expansion is fixed at $k_{\max}$, the time step is selected keeping in mind the accuracy of the evolution operator and the run time of the numerical simulation. The numerical stability is tested at each step by confirming whether the trace of the density matrix is 1 with an error less than 10^{-12}. In practice the polynomial method is much more efficient than that of the Runge-Kutta algorithm used in Ref. [42] under the same conditions of accuracy.

From the time evolved state $|\Psi_m(t)\rangle$, we can always obtain the density matrix $\rho(t)$ using (23). The reduced density matrix of the bipartite system can be calculated by tracing out the environment degrees of freedom

$$\rho_s(t) = \mathrm{Tr}_B\, \rho(t), \tag{27}$$

and can be expressed in the Hilbert space spanned by the orthonormal vectors $|11\rangle, |10\rangle, |01\rangle, |00\rangle$.

One of the interesting features is the steady-state behavior of quantum coherence. For the sake of illustration we consider the long-time limit of quantum coherence ($t \to \infty$) to describe the steady-state behavior of quantum coherence (see Fig. 1). From the plots we find that the quantum coherence increases logarithmically with an increase in the anisotropy parameter γ. On enhancing the spin-spin coupling ratio g_0/g, we observe from Fig. 1(b) that the coherence increases very rapidly satisfying a law $C_T \sim (g_0/g)^n$, $n \backsim 3$. Finally, in Fig. 1(c), we show the change in quantum coherence as a function of temperature. We find that the coherence initially increases and attains a maximal value and then slowly decays. The maximal value attained is a function of the anisotropy parameter and the higher the value of γ, the greater is the maximal value of coherence.

In the next section we investigate the dynamics of quantum coherence of the central spins considering different initial states. In all the numerical studies, we assume that $\mu_0 = 2g$ and $g = 1$, with the other parameters being varied.

V. DYNAMICS OF COHERENCE IN PURE STATES

In this section, we investigate the coherence dynamics of a two-qubit system due to an external environment for various pure initial states. The following three kinds of initial states are considered: (a) bipartite pure states initially containing only global coherence (e.g., Bell states); (b) bipartite pure state initially possessing only local coherence (e.g., coherent separable states); (c) bipartite pure states initially without any coherence (e.g., incoherent separable states).

A. Maximally entangled coherent states

The dynamics of quantum coherence in the two-qubit system is analyzed when the initial state is prepared in the form of Bell states. We investigate the dynamics of two Bell states $|\phi^+\rangle = (|00\rangle + |11\rangle)/\sqrt{2}$ and $|\psi^+\rangle = (|01\rangle + |10\rangle)/\sqrt{2}$, which are shown in Fig. 2. For the Bell states, the entire coherence in the system can be attributed to the global coherence distributed between the qubits. The local coherence is zero because the product state constructed from a Bell state is a completely incoherent state.

In Figs. 2(a) and 2(d), we show the variation of coherence with different anisotropy parameters for the states $|\phi^+\rangle$ and $|\psi^+\rangle$, respectively. From both the plots, we observe that the collapse and revival of coherence with large amplitudes is more pronounced for $\gamma = 0$ than for $\gamma = 1$, which is inde-

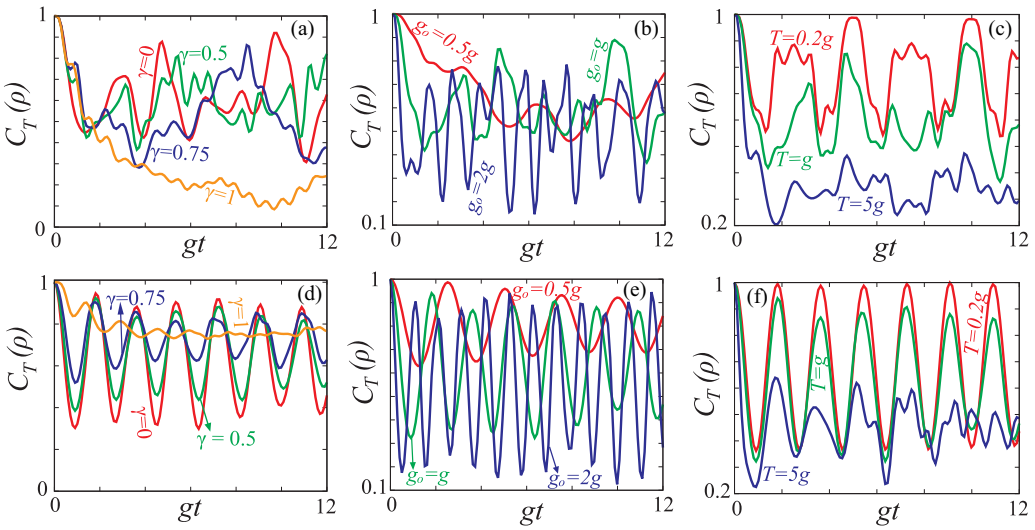

FIG. 2. Dynamics of quantum coherence of the two-qubit system initialized to the Bell states $|\phi^+\rangle = (|00\rangle + |11\rangle)/\sqrt{2}$ and $|\psi^+\rangle = (|01\rangle + |10\rangle)/\sqrt{2}$. We set $g_0 = g$ and $T = g$ and calculate the time evolution of quantum coherence for different values of γ as shown in (a) and (d) for the states $|\phi^+\rangle$ and $|\psi^+\rangle$, respectively. Similarly setting $\gamma = 0.25$ and $T = g$ we show the variation of the dynamics with respect to the parameter g_0 for $|\phi^+\rangle$ and $|\psi^+\rangle$ in (b) and (e), respectively. Finally, we show the temperature dependence of the dynamics of the states in (c) and (f) for $|\phi^+\rangle$ and $|\psi^+\rangle$ for the constant values $\gamma = 0.25$ and $g_0 = g$.

pendent of initial Bell states. It indicates that the increase of anisotropy of the bath and interaction leads to a smaller time to reach stable coherence. In contrast to the time evolution of entanglement in Ref. [31], the coherence is more robust. The time dynamics of coherence for various values of g_0 (the subsystem-bath interaction) is described in Figs. 2(b) and 2(e), respectively. The oscillatory frequency of coherence becomes much larger when the value of g_0 is increased. This is due to the fact that a higher value of g_0 implies a stronger interaction with the spin-star environment, which leads to a higher speed of exchange of information between the two-qubit subsystem and surrounding spin environment.

We also study the effect of temperature on the coherence dynamics. The corresponding results are shown for $|\phi^+\rangle$ and $|\psi^+\rangle$ in Figs. 2(c) and 2(f), respectively. It is observed that the revival of coherence for different temperatures happens, but the amount of coherence revived is dependent on the temperature of the bath. As the temperature increases, the degree of coherence revival decreases due to the decoherent effects of the temperature.

B. Coherent separable state

We now turn to the case of the two-qubit subsystem initialized to a separable state. In our discussion below, we look into the coherence dynamics of the following product state $|\chi\rangle = |++\rangle = (|00\rangle + |01\rangle + |10\rangle + |11\rangle)/2$, which is not entangled. The numerical results are shown in Figs. 3 and 4.

Since the two-qubit subsystem is coupled with a common bath, the state of the qubits becomes entangled in the course of evolution which can be measured through a numerical calculation of concurrence, an entanglement monotone [31–33]. Figure 3 shows the dynamics of the entanglement (E), total coherence (TC), local coherence (LC), and global coherence (GC) of the subsystem. From the plots it is seen that, while the entanglement and global coherence are initially zero, they attain a finite value during evolution and also have a similar time dependence. This is because of the interqubit correlations introduced in the quantum system by the common bath. We also should note that the entanglement disappears at $gt \approx 13$, but the global coherence generated always exists during the evolution. Meanwhile, the local coherence which initially takes its maximal value tends to decrease with time. The entanglement and local coherence have complementary behaviors, such that the entanglement increases when the local coherence decreases and vice versa. This indicates that local coherence is transferred to global coherence through the bath, and at particular times there is only interqubit correlation and entanglement between the two qubit, but no intraqubit coherence.

In Fig. 4, we show the global and local coherence for various values of the anisotropy parameter γ, system-bath

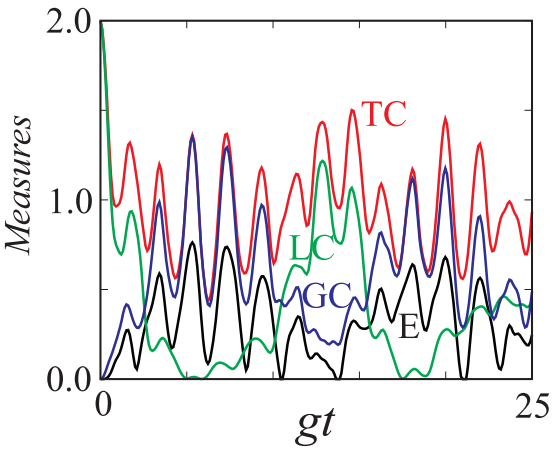

FIG. 3. Time evolution of entanglement (E), global coherence (GC), local coherence (LC), and total coherence (TC) for the state $|\chi\rangle$ with $\gamma = 0.25$, $g_0 = g$, and $T = g$.

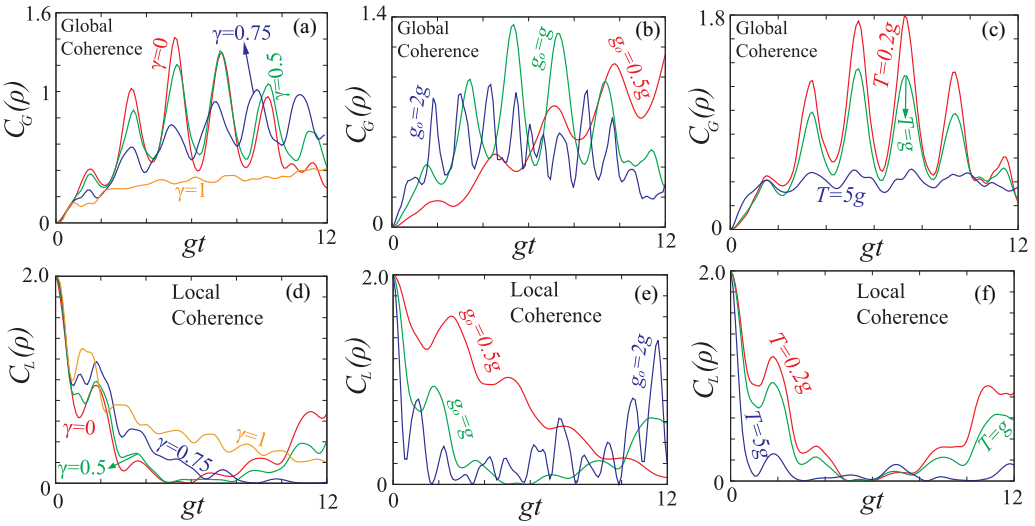

FIG. 4. Time evolution of global and local coherence for the state $|\chi\rangle$. In (a) and (d) we show the dynamics of global and local coherence respectively for different values of γ with the other parameters being maintained at $g_0 = g$ and $T = g$. For different values of g_0 we show the time variation of coherence for the global and local coherence in (b) and (e), respectively, keeping $\gamma = 0.25$ and $T = g$. The time variation of coherence is shown in (c) and (f) for the global and local coherence, respectively, with the values of $\gamma = 0.25$ and $g_0 = g$.

couplings g_0, and temperature T. We see from Fig. 4(a) that the global coherence is initially zero for all values of γ, but it increases with time, attains a maximum value, and again decreases. In the case of local coherence, the coherence is maximum initially, which falls to zero and then revives as observed in Fig. 4(d). For $\gamma = 0$ (the isotropic case), both the local coherence and the global coherence attain their maximum and minimum value compared with other values of the anisotropy parameter. Also the time taken for the fall and revival of coherence is longer for larger values of the anisotropy parameter. It indicates that the increase of anisotropy hinders the generation of global coherence and loss of local coherence for $|\chi\rangle$. For the system-bath coupling g_0, in Fig. 4(b) we see that the initial global coherence is always zero for any value of g_0 and is generated at a later time due to the interaction with the bath. While it initially increases, it again decreases and the rate of this change in coherence is entirely dependent on the value of g_0. The dynamics of local coherence is shown in Fig. 4(e). Its initial value is always the maximal value of 2, and it decreases and then revives. This change is also dependent on the value of g_0 and happens faster for higher values of the coupling g_0. The larger the value of g_0, the faster the change in coherence, because the subsystem and the bath interact more strongly when g_0 is higher. The transient dynamics of both the global coherence and local coherence for different temperatures is shown in Figs. 4(c) and 4(f). The global coherence which is initially zero increases and reaches a maximum value which is inversely proportional to the temperature as shown in Fig. 4(c). As for the local coherence it is initially at a finite value which reaches zero and then revives. This collapse and revival of coherence is dependent on the temperature and the maximum value of the coherence revived is inversely proportional to the temperature as displayed through Fig. 4(f). The amount of maximal coherence and the revived value of coherence is inversely proportional to the temperature because of the thermal decoherence effects. Therefore, the total coherence decreases with the temperature. In the present part, we do not consider the dynamics of the total coherence which is a sum of the local and global coherence. This is because the response of total coherence to the different interaction parameters such as γ, g_0, and T will be just an additive combination of the local and global effects.

C. Incoherent separable state

We now turn to examining the transient dynamics of quantum coherence for initially incoherent separable states. We consider the two initial states $|00\rangle$ and $|01\rangle$, which do not have any coherence since they have a diagonal density matrix (in the σ^z basis). As the two-qubit subsystem evolves in time, it gains coherence as can be observed from the plots in Fig. 5. From Figs. 5(a) and 5(c), we find that the maximum value of coherence is attained for $\gamma = 0$ in the case of $|01\rangle$ but for $\gamma = 1$ in the case of $|00\rangle$. The subsystem gains little coherence when $\gamma = 1$ for $|01\rangle$ as well as for $|00\rangle$. The variation of coherence with time for the different values of g_0, the system bath interaction parameters, is shown in Figs. 5(b) and 5(d) for the states $|00\rangle$ and $|01\rangle$, respectively. The increase of the coupling to the bath helps to increase the global coherence.

Throughout the entire dynamics the only coherence formed in the subsystem is the global coherence, which signals the introduction of only interqubit correlations. Hence, in Fig. 5, we show the dynamics of the total coherence, which is equal to the global coherence in this case. Thus we find that quantum coherence can be introduced in an incoherent state in contact with the common bath, an effect which can be described as bath-induced coherence. This is because the common bath introduces quantum correlations to the incoherent state, which manifests itself as coherence of the subsystem.

When we observe the dynamics of the Bell states $|\phi^+\rangle$ and $|\psi^+\rangle$ we can notice that $|\phi^+\rangle$ has a chaotic dynamics,

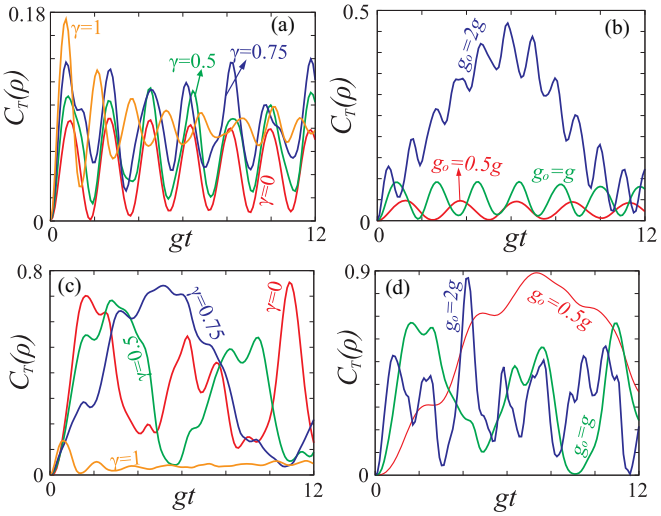

FIG. 5. Time evolution of the total coherence for the states $|00\rangle$ and $|01\rangle$. In (a) and (c) we show the dynamics of total coherence of the states $|00\rangle$ and $|01\rangle$ respectively for various values of γ fixing $g_0 = g$ and $T = g$. Setting $\gamma = 0.25$ and $T = g$ we show the dynamics of total coherence for states $|00\rangle$ and $|01\rangle$ in (b) and (d), respectively.

whereas in $|\psi^+\rangle$ the dynamics is more regular. In the case of the quantum state $|\phi^+\rangle$, the revival state is not exactly the same and hence the nature of the dynamics is chaotic, since the quantum state keeps changing throughout the evolution. The state $|\psi^+\rangle$ exhibits a periodic behavior since the revival state is close to $|\psi^+\rangle$. In contrast the state $|00\rangle$ has periodic dynamics, since its revival state is close to itself. However, the state $|01\rangle$ presents a rather chaotic dynamics since the quantum state changes throughout the evolution. The results which are well established for the entanglement and fidelity dynamics in Ref. [31] are also confirmed for the coherence dynamics through our present work.

From our investigations of the pure states, we should point out some interesting features. When the initial state is either the Bell state $|\phi^+\rangle$ and $|\psi^+\rangle$ or the incoherent state $|00\rangle$ and $|01\rangle$, we observe the dynamics of only global coherence. This is because the local coherence which is initially zero is never generated due to the interaction between the subsystem and the bath. Both the Bell states and the incoherent states belong to the class of states known as the X states in which the density matrix has elements only along the diagonal and the antidiagonal. It is well known [47] that under time evolution an X state will evolve into another X state. Further, it is also known that the product state corresponding to an X state $[\pi(\rho)]$ is diagonal and hence incoherent. Hence an X state contains only global coherence and since it always evolves into another X state [47], no local coherence is generated in its evolution. In the case of the separable state, the state $|\chi\rangle$ can be written in a product form and hence it does not have global coherence. But the product state is not necessarily diagonal, and local coherence can be present in the system. The interaction of the subsystem with the environment gives rise to quantum correlations between the two qubits. This quantum correlation generates the global coherence which does not exist in the initial system. Since the product state is not strictly an X state, there is a complex relationship between the X-state (diagonal and antidiagonal) elements and the remaining elements giving rise to the observed dynamics of the local and global coherence.

VI. DYNAMICS OF COHERENCE IN MIXED STATES

In this section, we explore the dynamics of quantum coherence when it is initially prepared in a mixed state. This is relevant from a practical point of view since it is generally difficult to prepare a perfectly pure state experimentally. We consider mixed states of the form

$$\rho_\Phi = \frac{1-\mu}{4} I_4 + \mu |\Phi\rangle\langle\Phi|, \tag{28}$$

where $|\Phi\rangle$ is a pure state and μ is the mixing parameter. Here I_4 is the maximally mixed two-qubit state and corresponds to a classically maximum entropy probability distribution. As such it has no quantum correlation and thus has zero quantum discord [1]. We present the results for the entangled, separable, and maximally mixed states below.

A. Werner Bell states

The time evolution of quantum coherence for the mixed state defined in (28) with $|\Phi\rangle = |\psi^+\rangle$ is shown in Figs. 6(a) and 6(b). For the values of the parameters $\gamma = 0.5$, $g_0 = g$, and $T = g$, we show the total coherence dynamics in Fig. 6(a) for various values of the mixing parameter μ. We observe that the amount of coherence generally increases with the mixing parameter, as expected for a state of higher purity.

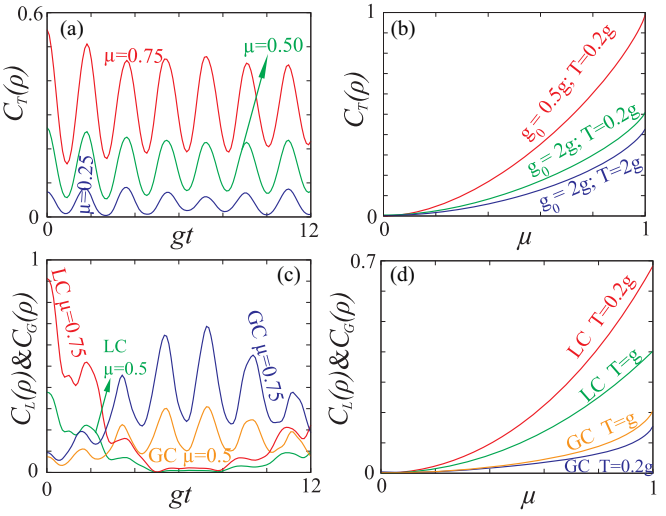

FIG. 6. Time evolution of quantum coherence from an initially mixed state of Werner form given in (28), for $|\psi^+\rangle$ and $|\chi\rangle$ states. (a) For the state $|\psi^+\rangle$, we display the total coherence dynamics for different values of the mixing parameter μ setting $\gamma = 0.5$, $g_0 = g$, and $T = g$. (b) At a fixed time $gt = 5$ we show the monotonic change of the coherence with the mixing parameter fixing $\gamma = 0.75$, the values of g_0 and T being shown in the plot. (c) For the mixed state with $|\chi\rangle$ we investigate the time dynamics of global and local coherence for $\gamma = 0.5$, $g_0 = g$, and $T = g$. (d) The variation of coherence with μ at a fixed time $gt = 5.0$ is given for $\gamma = 0.75$ and $g_0 = g$ for different values of temperature.

It is because the quantum coherence is present only for the Bell state, and is zero for a completely mixed state $I_4/4$. It is known from past studies that the Werner-Bell state (28) has nonzero entanglement in the range $\mu > 1/3$, and hence for $0 \leqslant \mu \leqslant 1/3$ the state has no entanglement [48]. The global quantum coherence is a consequence of both quantum correlations due to entanglement and interqubit quantum correlations (i.e., quantum discord). Therefore, the global quantum coherence is nonzero even when the state is separable. We demonstrate the variation of coherence as a function of the mixing parameter μ for fixed values $gt = 5$ and $\gamma = 0.75$, and for various choices of spin-bath coupling parameter g_0 and temperature T in Fig. 6(b). We see that the coherence increases monotonically with increasing the mixing parameter for all parameter choices.

B. Separable mixed state

We now consider the separable state $|\Phi\rangle = |{+}{+}\rangle$ in (28) as the initial condition for the time-dependent coherence dynamics. Such a quantum state presents very rich time dynamics since the evolution causes a change in both global and local coherence of the system. Selecting a fixed value of parameters $\gamma = 0.5, g_0 = g, T = g$, we examine the dynamics for different values of μ in Fig. 6(c). We find that the coherence dynamics is more subdued for both the local and global coherence with the decrease in the mixing parameter μ. The reason is that we are mixing the separable state with a classical correlated state. For a fixed value of $gt = 5$ with $\gamma = 0.75$ and $g_0 = 2g$ we also find the variation of local and global coherence with the mixing parameter in Fig. 6(d). The calculation is carried out for different values of the temperature for the sake of consistency. We find that both local and global coherence displays monotonic decrease with *decreasing* mixing parameter μ. Also we can observe finite temperature decoherence effects in the dynamics of local and global coherence.

C. Maximally mixed incoherent state

We finally consider the maximally mixed state corresponding to $\mu = 0$ in (28). This state has zero purity and is incoherent for any basis choice. The time dynamics of this state for various parameters are shown in Fig. 7. Naively, one might expect that a maximally mixed state would be invariant to any time dynamics because it has no coherence. In Fig. 7(a), the time variation of coherence is shown for $g_0 = 2g$ and $T = g$ with various values of the anisotropy parameter. Contrary to the naive expectation, the total coherence is initially zero, but starts to increase after the system interacts with the bath and reaches a finite value and then decreases. The maximal value attained depends on the anisotropy parameter and is higher for the isotropic situation when $\gamma = 0$ and is the least for $\gamma = 1$, the transverse field Ising model. Analogously, we see, in Fig. 7(b), that when the value of spin-bath interaction g is increased, the coherence dynamics becomes more prominent. The reason is that a higher value of g implies a stronger interaction between the bath and the system and hence the coherence is generated by interacting with the environment.

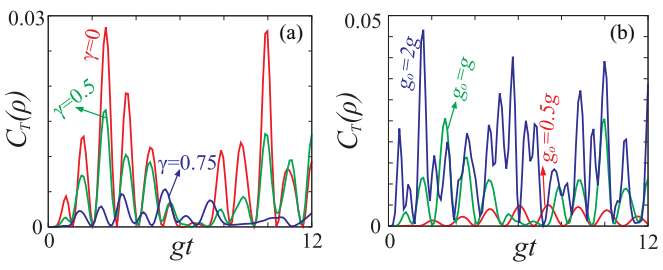

FIG. 7. Time dynamics of the initially maximally mixed state $I_4/4$. (a) Time evolution of the total coherence for various anisotropy parameters γ, setting $g_0 = 2g$ and $T = g$. (b) Time evolution of the total coherence for various system-bath couplings g_0, setting $\gamma = 0.25$ and $T = g$.

The knowledge on the coherence dynamics of the mixed states leads us to similar results for the case of X-type state. Both the Werner-Bell state and the maximally mixed state are X states and hence we observe only the time evolution of global coherence. No local coherence exists or is generated in the system throughout the course of evolution. This is because any given X-state evolves only into another X state [47] and such states have a product form which always has a diagonal density matrix, and is incoherent. Therefore, there is no generation of local coherence since it needs the product states to be nondiagonal. In the case of an initially mixed separable state, the local coherence is much more dominant than the global coherence. Due to the interaction with the environment, the global coherence of the state increases, leading to the dynamics of local and global coherence observed in the present work. For the case of maximally mixed state we find that it initially does not have any coherence, but later on there is coherence introduced in the system by the environment. We find that the maximal value of coherence is far smaller (typically one order of magnitude) than the amount of coherence introduced in other states. This is because the entire coherence gained by the maximally mixed state which is classically correlated comes from its interaction with the environment which is quantum by nature. On increasing the temperature the quantum nature of environment decreases and so the amount of coherence introduced by the bath decreases and becomes negligible at high temperatures. On the contrary the pure incoherent states $|00\rangle$ and $|01\rangle$ possess a higher amount of coherence generated during the course of the transient dynamics. It is noticed that these states have a purity equal to one, while the maximally mixed state has zero purity. Such states have the opportunity to convert their inherent quantum property (i.e., purity) into coherence during the course of evolution, while maximally mixed states do not have this opportunity, and can only become coherent unless coherence is introduced externally. To illustrate this point we compare the dynamics of coherence and purity. Using Eq. (14), we measure the quantum coherence of the states $|00\rangle$ and $|01\rangle$. The connection between purity and quantum coherence of a system has been investigated through several works [49,50]. The purity of a quantum state is measured as its distance to the maximally mixed state. Using the relative entropy distance measure, the purity of a quantum system is

$$P = S(\rho \| I_d/d) \equiv \log_2 d - S(\rho_s), \tag{29}$$

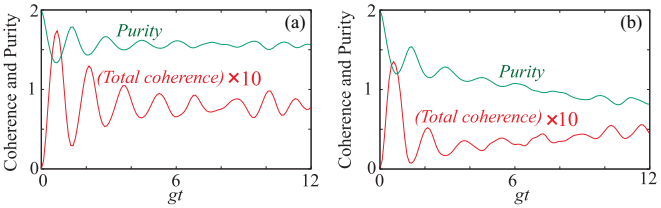

FIG. 8. Time dynamics of total quantum coherence and purity of the system for the (a) $|01\rangle$ and (b) $|00\rangle$ quantum states. The value of the parameters used are $\gamma = 1$, $T = g$, and $g_0 = g$. The values of coherence are multiplied by 10.

where P is the purity and d is the dimension of the Hilbert space. From the plots (see Fig. 8), we observe that initially the coherence is zero and the purity is at a maximal value. Then the loss of purity is accompanied by an increase in quantum coherence of the system. The purity and coherence exhibits complementary dynamics, where increase (decrease) of one quantity is accompanied by the decrease (increase) of the other. This gives credence to our point that the purity can be converted to quantum coherence in a given quantum system.

D. Central spins in a finite bath

In our work so far we have studied the dynamics of quantum coherence of a two qubit system exposed to an infinite spin bath. Hence it is natural to ask the question as to what is the dynamics of coherence when the number of spins in the bath is finite. To answer this question we investigate the dynamics of coherence in the entangled states $|\phi^+\rangle$ and $|\psi^+\rangle$ as well as in the incoherent separable states $|00\rangle$ and $|01\rangle$ for a bath size of $N = 40$ spins. The results are shown in Fig. 9.

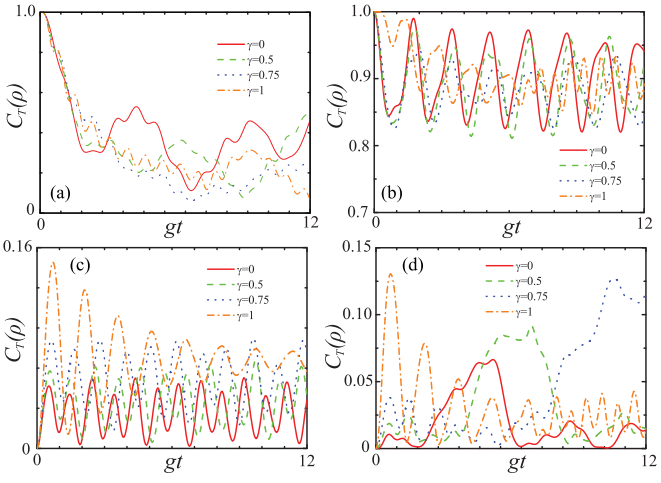

FIG. 9. Dynamics of quantum coherence of the two-qubit system initialized to the Bell states $|\phi^+\rangle = (|00\rangle + |11\rangle)/\sqrt{2}$ and $|\psi^+\rangle = (|01\rangle + |10\rangle)/\sqrt{2}$ for $N = 40$. We set $g_0 = g$ and $T = g$ and calculate the time evolution of quantum coherence for different values of γ as shown in (a) and (b) for the states $|\phi^+\rangle$ and $|\psi^+\rangle$, respectively. In (c) and (d) we show the dynamics of total coherence of the states $|00\rangle$ and $|01\rangle$ respectively for various values of γ fixing $g_0 = g$ and $T = g$.

The coherence in the state $|\phi^+\rangle$ is initially at a maximal value and then it starts decreasing with time. It decreases to a minimal value and then revives again. The minimal value attained is lower for higher values of the anisotropy parameter γ. However, we notice that the dynamics of the state is chaotic. In the case of the state $|\psi^+\rangle$, there is also a fall and revival of coherence and the extremal values are higher for smaller values of the anisotropy parameter. The periodicity is also well marked for the lower values of the anisotropy parameter. The state $|\phi^+\rangle$ is not very periodic, whereas the state $|\psi^+\rangle$ has a nice periodic behavior. This is because in $|\phi^+\rangle$ the revived state is not close to that of the original state [31] and so the dynamics is chaotic. But in $|\psi^+\rangle$ the original state and revived state are closer to each other [31] and so the dynamics is periodic in nature.

The quantum state $|00\rangle$ is initially incoherent and is also a separable state. But on interacting with the bath, the system gains coherence and this coherence exhibits a periodic dynamics. The amount of coherence gained depends on the anisotropy parameter and is higher for higher values of γ. Similarly, the state $|01\rangle$ is also an incoherent inseparable state, but on evolution it exhibits a chaotic dynamics. The amount of coherence gained is higher for higher values of γ. The state $|00\rangle$ is periodic because the revived state is closer to the original state, but the state $|01\rangle$ is chaotic because the revival state is not closer to the original state. Comparing these results with the ones corresponding to those for the infinite bath system, we find that the results agree qualitatively with each other. Hence we claim that our results which have been discussed for quantum systems in an infinite bath also hold qualitatively when the systems are in a finite bath.

VII. SUMMARY AND CONCLUSIONS

An investigation of the time dynamics of quantum coherence of two central spins in a finite temperature external environment was carried out. The dynamics were investigated for a variety of initial conditions of the two central spins, from pure to mixed states. For pure states we consider the Bell state and a coherent and incoherent separable state. The mixed state properties were explored through the study of Werner-Bell state, the mixed separable state, and the maximally mixed state. The coherence was decomposed into its local and global coherence contributions to analyze the origins of the coherence. Also the time evolution was examined by varying important parameters like the anisotropy of the spin interaction and the interaction strength between the bath and the central spin, as well as the temperature. From our investigation we notice that the Bell state $|\psi^+\rangle$ presents a dynamics which is more regular compared to the dynamics of the Bell state $|\phi^+\rangle$. This is because the revival state of the $|\psi^+\rangle$ is closer to the initial state and hence it gives rise to periodic dynamics. In the case of $|\phi^+\rangle$, the revival state is not the same as the initial state and hence it has chaotic dynamics. Similarly in the case of the separable states, the state $|01\rangle$ exhibits a chaotic dynamics since its revival state is not the same as the initial state. But the quantum state $|00\rangle$ has a much more periodic behavior since the revival state is close to the initial state. Hence the periodicity or its lack thereof depends on how close the revival state is to the initial state. While the

results have been investigated for systems in contact with an infinite bath, we also establish that similar qualitative results hold for systems in contact with a finite number of spins. (See Fig. 9.)

From the numerical results corresponding to the mixed Bell states and mixed separable state we notice that all kinds of coherence decrease on mixing with incoherent states. Further in the case of Werner-Bell states we find that the coherence is also present at values less than $\mu = 1/3$, which is the standard Werner separability criteria. In the case of the Werner-Bell state the total coherence is equal to the global coherence since the entire correlations are due to interqubit correlations. Below the Werner separability criteria $\mu < 1/3$, the global coherence can be attributed to the presence of quantum correlations, in agreement with the results that the quantum discord is nonzero for any $\mu > 0$. We also showed that, at a fixed time step, the coherence decreases monotonically with decreasing the mixing parameter for both the Werner-Bell state and the mixed separable state. Finally, as expected the thermal effects present an overall decoherence effect on the dynamics of the central subsystem.

The observations of the dynamics of quantum coherence give rise to the following conclusions. (i) An X state will always have global coherence. The reason is a combination of two factors, namely an X state will always evolve into an X state and the product form of the X state is always diagonal in nature and is therefore incoherent. We demonstrate this result by the calculations of the Bell states, incoherent states $|00\rangle, |01\rangle$, Werner-Bell states, and the maximally mixed states. (ii) A state with only initial local coherence gains global coherence during the course of evolution. This is because the interaction between the two-qubit subsystem and the common bath creates interqubit correlations, which give rise to the global coherence between the two qubits. (iii) It is possible for a completely incoherent state to gain coherence by interacting with an external bath. Here we note that there are two ways through which an incoherent state can gain coherence: one is by interacting with the external bath and the second is through an interconversion of other quantum properties into coherence. One such convertible quantum feature is the purity of the system and through the course of dynamical evolution part of the purity might get converted into coherence. A comparison between the pure incoherent states $|00\rangle, |01\rangle$ and the maximally mixed state shows that, while both these states gain global coherence during evolution, the amount of coherence gained in the pure incoherent states is much larger (typically one order of magnitude) than that gained by the maximally mixed state. In the pure incoherent state both the interaction with the external bath and the interconversion of purity creates the global coherence. But in the case of the maximally mixed state the only source of coherence is the correlation with the environment. To illustrate it further we calculate the purity and coherence of the quantum states $|01\rangle$ and the state $|00\rangle$, where we notice the complementary dynamics of purity and coherence. We note that, in Ref. [51], an experimental interconversion between coherence and quantum correlations was demonstrated through the use of ancillary qubits. In the present work we showed the possibility of interconversion between coherence and purity of a system by subjecting the system to a time evolution process. An experimental demonstration of such interconversion would be very interesting in our opinion. An interesting extension of the current work will be to describe the dynamics of coherence and its distribution in systems with more than two spins, which would lead to more complex behavior.

ACKNOWLEDGMENTS

Z.L. is supported by National Natural Science Foundation of China (Grants No. 11774226 and No. 61927822). J.J. is supported by National Natural Science Foundation of China (Grants No. 11575071 and No. 11974311). R.C. and T.B. are supported by the Shanghai Research Challenge Fund, New York University Global Seed Grants for Collaborative Research, National Natural Science Foundation of China (Grants No. 61571301 and No. D1210036A), the NSFC Research Fund for International Young Scientists (Grants No. 11650110425 and No. 11850410426), NYU-ECNU Institute of Physics at NYU Shanghai, the Science and Technology Commission of Shanghai Municipality (Grant No. 17ZR1443600), the China Science and Technology Exchange Center (Grant No. NGA-16-001), and the NSFC-RFBR Collaborative grant (No. 81811530112).

[1] H. Ollivier and W. H. Zurek, Phys. Rev. Lett. **88**, 017901 (2001).
[2] L. Henderson and V. Vedral, J. Phys. A: Math. Gen. **34**, 6899 (2001).
[3] T. Baumgratz, M. Cramer, and M. B. Plenio, Phys. Rev. Lett. **113**, 140401 (2014).
[4] P. Skrzypczyk, M. Navascués, and D. Cavalcanti, Phys. Rev. Lett. **112**, 180404 (2014).
[5] A. Grudka, K. Horodecki, M. Horodecki, P. Horodecki, R. Horodecki, P. Joshi, W. Kłobus, and A. Wójcik, Phys. Rev. Lett. **112**, 120401 (2014).
[6] L.-H. Shao, Z. Xi, H. Fan, and Y. Li, Phys. Rev. A **91**, 042120 (2015).
[7] S. Rana, P. Parashar, and M. Lewenstein, Phys. Rev. A **93**, 012110 (2016).
[8] C. Radhakrishnan, M. Parthasarathy, S. Jambulingam, and T. Byrnes, Phys. Rev. Lett. **116**, 150504 (2016).
[9] C. Napoli, T. R. Bromley, M. Cianciaruso, M. Piani, N. Johnston, and G. Adesso, Phys. Rev. Lett. **116**, 150502 (2016).
[10] A. E. Rastegin, Phys. Rev. A **93**, 032136 (2016).
[11] D. Girolami, Phys. Rev. Lett. **113**, 170401 (2014).
[12] X. Yuan, H. Zhou, Z. Cao, and X. Ma, Phys. Rev. A **92**, 022124 (2015).
[13] X.-D. Yu, D.-J. Zhang, G. F. Xu, and D. M. Tong, Phys. Rev. A **94**, 060302(R) (2016).
[14] C. Radhakrishnan, M. Parthasarathy, S. Jambulingam, and T. Byrnes, J. Phys.: Conf. Ser. **752**, 012003 (2016).
[15] B. Opanchuk, L. Rosales-Zárate, R. Y. Teh, and M. D. Reid, Phys. Rev. A **94**, 062125 (2016).

[16] Q. Zheng, J. Xu, Y. Yao, and Y. Li, Phys. Rev. A **94**, 052314 (2016).
[17] G. Karpat, B. Çakmak, and F. F. Fanchini, Phys. Rev. B **90**, 104431 (2014).
[18] A. L. Malvezzi, G. Karpat, B. Çakmak, F. F. Fanchini, T. Debarba, and R. O. Vianna, Phys. Rev. B **93**, 184428 (2016).
[19] C. Radhakrishnan, M. Parthasarathy, S. Jambulingam, and T. Byrnes, Sci. Rep. **7**, 13865 (2017).
[20] C. Radhakrishnan, I. Ermakov, and T. Byrnes, Phys. Rev. A **96**, 012341 (2017).
[21] T. D. Ladd, F. Jelezko, R. Laflamme, Y. Nakamura, C. Monroe, and J. L. O'Brien, Nature (London) **464**, 45 (2010).
[22] A. P. Alivisatos, Science **271**, 933 (1996).
[23] D. Loss and D. P. DiVincenzo, Phys. Rev. A **57**, 120 (1998).
[24] M. G. Dutt, L. Childress, L. Jiang, E. Togan, J. Maze, F. Jelezko, A. Zibrov, P. Hemmer, and M. Lukin, Science **316**, 1312 (2007).
[25] J. Schliemann, A. Khaetskii, and D. Loss, J. Phys.: Condens. Matter **15**, R1809 (2003).
[26] S. Paganelli, F. de Pasquale, and S. M. Giampaolo, Phys. Rev. A **66**, 052317 (2002).
[27] M. Lucamarini, S. Paganelli, and S. Mancini, Phys. Rev. A **69**, 062308 (2004).
[28] A. Hutton and S. Bose, Phys. Rev. A **69**, 042312 (2004).
[29] Y. Hamdouni, M. Fannes, and F. Petruccione, Phys. Rev. B **73**, 245323 (2006).
[30] X.-Z. Yuan, H.-S. Goan, and K.-D. Zhu, Phys. Rev. B **75**, 045331 (2007).
[31] J. Jing and Z.-G. Lü, Phys. Rev. B **75**, 174425 (2007).
[32] J. Jing, Z.-G. Lü, and G.-H. Yang, Phys. Rev. A **76**, 032322 (2007).
[33] J. Jing, Z. Lü, and H.-R. Ma, Mod. Phys. Lett. B **23**, 911 (2009).
[34] A. Imamoglu, D. D. Awschalom, G. Burkard, D. P. DiVincenzo, D. Loss, M. Sherwin, A. Small *et al.*, Phys. Rev. Lett. **83**, 4204 (1999).
[35] S.-B. Zheng and G.-C. Guo, Phys. Rev. Lett. **85**, 2392 (2000).
[36] X. Wang, Phys. Rev. A **64**, 012313 (2001).
[37] D. A. Lidar and L.-A. Wu, Phys. Rev. Lett. **88**, 017905 (2001).
[38] K. C. Tan, H. Kwon, C.-Y. Park, and H. Jeong, Phys. Rev. A **94**, 022329 (2016).
[39] H.-P. Breuer, D. Burgarth, and F. Petruccione, Phys. Rev. B **70**, 045323 (2004).
[40] H.-P. Breuer, Phys. Rev. A **69**, 022115 (2004).
[41] T. Holstein and H. Primakoff, Phys. Rev. **58**, 1098 (1940).
[42] L. Tessieri and J. Wilkie, J. Phys. A: Math. Gen. **36**, 12305 (2003).
[43] H. Tal-Ezer and R. Kosloff, J. Chem. Phys. **81**, 3967 (1984).
[44] S. K. Gray, J. Chem. Phys. **96**, 6543 (1992).
[45] X.-G. Hu, Phys. Rev. E **59**, 2471 (1999).
[46] J. Jing and H. R. Ma, Phys. Rev. E **75**, 016701 (2007).
[47] T. Yu and J. Eberly, Quantum Inf. Comput. **7**, 459 (2007).
[48] C. H. Bennett, G. Brassard, S. Popescu, B. Schumacher, J. A. Smolin, and W. K. Wootters, Phys. Rev. Lett. **76**, 722 (1996).
[49] A. Streltsov, H. Kampermann, S. Wölk, M. Gessner, and D. Bruß, New J. Phys. **20**, 053058 (2018).
[50] C. Radhakrishnan, Z. Ding, F. Shi, J. Du, and T. Byrnes, Ann. Phys. (NY) **409**, 167906 (2019).
[51] K.-D. Wu, Z. Hou, Y.-Y. Zhao, G.-Y. Xiang, C.-F. Li, G.-C. Guo, J. Ma, Q.-Y. He, J. Thompson, and M. Gu, Phys. Rev. Lett. **121**, 050401 (2018).